Original Research Article

Evaluation of Wavelet Orthogonal Frequency Division Multiplexing Massive MIMO (W-OFDM mMIMO) for Enhancing Spectral and Energy Efficiencies in Digital Wireless Communication System

ABSTRACT

Research into cutting-edge systems that can satisfy the rising needs for greater data rate and increased reliability is becoming more and more necessary as wireless communication technologies continue to evolve. To enhance the spectral and energy efficiencies, this study examine the performance of massive multiple input multiple output (mMIMO) communication systems using wavelet-order orthogonal frequency division multiplexing (W-OFDM). Also, a communication system was created based on W-OFDM Massive MIMO using MATLAB to model its operation. The simulated system's various stages of operation was examined through detailed analysis and its performance was compare with prior studies and practical networks on OFDM. Key performance metrics, specifically the data throughput, was evaluated to assess the effectiveness and viability of the system. The simulation results indicates that W-OFDM can achieve up to 35% reduction in peak-to-average-power-ratio (PAPR) compared to the traditional OFDM, with a 20% improvement in BER performance under Rayleigh fading conditions. Also, the spectral efficiency of W-OFDM mMIMO outperforms convectional OFDM by 15%, making it a viable technology for future communication networks requiring high data rates and reliability. This implies that, the analytical evaluation confirms that W-OFDM mMIMO provides substantial benefits for improving energy and spectral efficiencies in wireless communication systems, addressing the challenges of increased user demands for high spectrum. This study contributes to the understanding of MIMO systems' performance optimization, highlighting the importance of antenna configuration and cell distance. Comprehensive analysis of spectral efficiency and energy efficiency trade-offs in MIMO systems and identification of optimal antenna configuration for maximum energy efficiency, addressing some of the challenges of future wireless communication systems.

Keywords: 5G network, W-OFDM, mMIMO, FFT-OFDM, antennal array, MATLAB

1. INTRODUCTION

The need for continuous advancement in communication technology infrastructure is to allow people and things (places, gadgets, etc.) to connect and communicate with one another in both real and virtual spaces (Guo, 2014). It is the foundation of a more intelligent era where robotics and artificial intelligence will permeate every aspect of our daily lives. Terré *et al*. (2013) predicts that communication technology will continue to advance swiftly in order to connect people with machines and objects through an ever-increasing exchange of information. In order to facilitate a multitude of new services, such as vehicle-to-vehicle communication, smart factories, and high-quality communication services, 5G technologies are being integrated into the fundamental infrastructure of many different industries (Terré *et al.*, 2013). Additionally, a new generation of connectivity technologies called ultra-wideband (UWB) is beginning to interconnect several devices and provide location-based services. Distances can be accurately and safely calculated with UWB technology. Communication technology, which is the backbone of the future society, is evolving at a faster rate and in order to prepare for it, more advance technologies have to be adopted.

In data communications and networking, orthogonal frequency-division multiplexing (OFDM) is a method of digital data modulation, whereby a single stream of data is divided into several separate sub-streams for transmission via multiple channels (Stuber *et al.*, 2004). It uses the principle of frequency division multiplexing (FDM), where the available bandwidth is divided into a set of sub-streams having separate frequency bands. When any signal is modulated by the sender, its sidebands spread out either side. A receiver can successfully demodulate the data only if it receives the whole signal. In case of FDM, guard bands are inserted so that interference between the signals, resulting in cross-talks, does not occur. However, since orthogonal signals are used in OFDM, no interference occurs between the signals even if their sidebands overlap. So, guard bands can be removed, thus saving bandwidth. The criteria that need to be maintained is that the carrier spacing should be equal to the reciprocal of the symbol period (Terry & Heiskala, 2002).

Massive MIMO is a technology that uses many antennas to multiplex messages for various devices on each time frequency source. The radiated energy is directed towards the desired directions while simultaneously minimizing intra- and inter-cell interference (Chataut & Akl, 2020). In a Massive MIMO system, the number of antennas at the base station is far greater than the total number of devices per signaling resource (Marzetta, 2010). Massive MIMO has been shown to preserve information rate and reduce base station radiated power by a factor proportional to the square root of the total number of deployed antennas, all while maintaining energy efficiency (Ngo *et al.*, 2014). Wavelet analysis is based on breaking down signals into scaled and shifted forms of a wavelet, whereas Fourier analysis breaks down signals into sine waves at particular frequencies. A wavelet is a wave-like oscillation that decays quickly as opposed to a sine wave. Wavelets can thus represent data on a variety of scales (Donzelli *et al.*, 2007). Wavelets are particularly useful for studying signals with both temporal and frequency components because of a special property that enables them to simultaneously capture both local and global information in a signal. Wavelets' fundamental concept is to use a collection of fundamental functions that are localized in both time and frequency to represent a signal (Zhang & Zhang, 2019). Recent advancements have been made in OFDM and Massive MIMO technologies, especially with 5G developments, which highlight critical innovations, addressing performance and deployment challenges (Agboje *et al.,* 2017). Cell-free Massive MIMO-OFDM systems have emerged as a promising solution, offering benefits such as enhanced asynchronous reception and improved spectral efficiency in dense urban areas (Ahmad & Shin, 2023). This approach can mitigate the limitations of conventional cell-based architectures by distributing antennas across an area without predefined cells, resulting in reduced interference and improved performance. Additionally, advances in wavelet-based OFDM have shown increased robustness against multipath fading compared to FFT-OFDM, making it advantageous in complex environments.

The rapid evolution of communication systems and the need for more efficient and reliable technologies to handle the growing data demands of modern networks have informed this study. Traditional OFDM methods, while effective, often face limitations in energy efficiency, spectral efficiency, and area power consumption, especially when deployed on a massive scale, as seen in Massive MIMO (mMIMO) systems. Emerging challenges such as high power requirements and interference issues in dense networks prompted the exploration of alternative techniques, such as Wavelet-OFDM, which potentially offers improvements over the widely used FFT-OFDM. In view of the above, the current research work aims at enhancing energy and spectral efficiencies of the communication system using wavelet-orthogonal frequency division multiplexing (W-OFDM) massive (mMIMO) technology. The study is significant because wavelets have proven to be advantageous in nearly every facet of digital wireless communication systems, encompassing data compression, transceiver design, source and channel coding, signal de-noising, and channel modeling. The main characteristic of wavelets in these applications is their flexibility and ability to accurately characterize signals. The convergence of communication and information technologies, along with the potential for widespread connectivity, has presented a problem in the development of architectures and technologies that can manage massive amounts of data while severely limiting resources like power and bandwidth. With the addition of Massive MIMO technology in this study, the wavelet transform will provide greater flexibility in creating the pulse's shape. These two technologies have significantly improved data throughput, low energy consumption, and spectral efficiency. This research seeks to provide a basis for future improvements in OFDM-based mMIMO systems, aligning with the demands of next-generation networks and advancing the field of wireless communication technology.

2. METHOD

The methods adopted in the study include the system channel model and linear processing using Zero Forcing Method with the help of MATLAB version R2018a and the HP ProBook 6550b version Laptop. The system design itself will be using the various power parameters.

2.1 KPI Requirements for Energy Efficiency in Communication System

The key performance indicators (KPIs) are specific, measurable, and quantifiable performance metrics used to track progress over time towards a particular objective or goal for (Marr, 2012). Monitoring KPIs, enables us to identify areas of strength and weakness, make data-driven decisions, and take actions to optimize performance. Energy and spectral efficiencies and data throughput are the three main KPIs that are considered for simulation in this study since the exponential growth of wireless communication calls for energy efficient solutions. Gartner in 1998 predicted that by 2015, mobile will surpass the PC as the most common web access device and consequently, more wireless infrastructure is needed to significantly increase the energy efficiency (Marr, 2012).

Energy Efficiency: This metric quantifies how efficiently energy is used to transmit data. To get the energy consumption of the entire network it is importance to take note of the energy consumption of the different network elements (Boccardi *et al.*, 2016). The operational energy consumption of the wireless network is divided into the RF (small fraction) and the overhead energy (the majority). It is the energy used to power up the circuits, baseband processing, transceivers and other supporting equipment like cooling and so on (Marr, 2012). With growing concerns over environmental impact and operational costs, energy efficiency is critical in network design. It ensures that networks can handle high data demands without excessive power consumption, which is especially important for applications in IoT and green communications. Energy efficiency is expressed as:

$$\mathrm{EE} = \frac{\text{overall data rate}}{\text{Total power consumed}} = \frac{\mathrm{R_T}}{P_\mathrm{T}} \text{ (bits/joule or bps/W)} \tag{1}$$

This metric has been applied in the current 4G network and is also applicable for the current 5G network (Badic *et al.*, 2010). In high-density networks like 5G and future 6G, where massive MIMO and complex beamforming are used, improving energy efficiency will help maintain network performance while minimizing environmental impact and cost. The metric is very simple but then it does not include network coverage so as a result, it cannot be utilized when trying to access energy efficiency of networks that have different coverage areas.

Area Power Consumption (APC): Refers to the amount of power consumed over a specific geographical area covered by a cellular network. This measure helps assess the total energy footprint of a network relative to its coverage area. The APC of a network can be gotten by dividing the network average power consumption by the average area covered by the network (Wang *et al.*, 2006). It is measured in watts per square kilometer as follows:

$$P = \frac{p}{A} \quad (W/km^2) \qquad (2)$$

Where the area power consumption is represented by ρ, P represents the average power consumption while A, represents the average cell coverage area. This metric is used for the comparison of power consumption in heterogeneous networks with varying site density. It is especially useful under low load conditions whereby we have the network limited by coverage. For widespread deployment in urban and rural areas, APC helps in comparing network deployments in terms of both energy and cost-efficiency. Higher power consumption in large areas can lead to sustainability challenges, and APC provides insights for more energy-aware infrastructure planning. As operators extend coverage in suburban and rural areas, measuring and minimizing APC is vital for creating scalable, efficient networks that can serve diverse geographies without excessive energy use.

Area Energy Efficiency (AEE): This is an extension of the bit per Joule metrics having an inclusion of network coverage area. It is used to determine the energy efficiency of a network with respect to its size (Wang *et al.*, 2015), The AEE is defined as the bit/Joule/unit area which a cell can support. It is mathematically expressed as:

$$AEE = \frac{EE}{A} \quad (bit/joule/m^2) \qquad (3)$$

Energy Consumption Gain (ECG): This is a metric used to compare the ECR of two systems. One system is used as the reference system while the other system is the one that its energy efficiency needs to be accessed. It is expressed mathematically as:

$$ECG = \frac{E_a}{E_b} \qquad (4)$$

E_a is the energy consumption of the reference system where E_b is the energy consumption of the system to be tested.

Energy Reduction Gain (ERG): This metric is derived from ECG metric, it is usually defined as:

$$ERG = 1 - \frac{1}{ECG} X100\% \qquad (5)$$

Spectral Efficiency (SE): Spectral efficiency in wireless communication measures how efficiently the available bandwidth is used to transmit data. It quantifies the rate of data transmission per unit bandwidth while maintaining reliable communication. Spectral efficiency is expressed in bits per second per Hertz (bps/s/Hz). SE is a cornerstone in maximizing the data-carrying capacity of wireless networks, particularly in dense urban areas where bandwidth is a limited resource. Efficient spectrum use allows networks to handle more users and services without increasing bandwidth requirements. Given the limited frequency spectrum available, spectral efficiency ensures that network operators can meet high data demands, which is critical for 5G networks that support diverse, high-throughput applications.

In a MIMO system, spectral efficiency improves due to spatial multiplexing. Assuming there are Nt transmits antennas and Nr receive antennas, the channel can be modeled as a matrix H, and the capacity depends on the eigenvalues of H. For MIMO, the spectral efficiency is given as:

$$\eta = \sum_{k=0}^{\min \mathrm{Nt,\, Nr}} \log(1 + \lambda i \cdot \mathrm{SNR}) \qquad (6)$$

where λ_i are the eigenvalues of the channel matrix H^H H (Hermitian transpose times H) and SNR is the signal-to-noise ratio.

System Channel Model and Linear Processing: The M antennas at the base station (BS) are spaced apart randomly that the channel components between the BS antennas and the single-antenna user equipment (UEs) are uncorrelated. The channel vector $\mathbf{h_k}$ is $[\mathbf{h}_{k,1}, \mathbf{h}_{k,2}, \ldots, \mathbf{h}_{k,M}]^T$ €C^{Mx1} which has entries$\{\mathbf{h}_{k,n}\}$ that describe the propagating channel between the n^{th} antenna at the BS and the k^{th} UE. Rayleigh small-scale fading is assumed for the distribution such that $\mathbf{h}_k$ ~ CN ($\mathbf{0}_M$, $\lfloor$ ($\mathbf{x}_k$) $\mathbf{I}_m$) this is a valid model for both small and large arrays. The Linear processing that is used for uplink data detection and downlink data precoding is Zero Forcing (ZF). For simplicity of the design, we assume that the BS is able to acquire perfect channel state information (CSI) from the uplink pilots.
G is used to denote the uplink linear receive combining matrix, which is made up of $[\mathbf{g}_1, \mathbf{g}_2, \ldots, \mathbf{g}_k]$ € C^{Mxk} with the column $\mathbf{g}_k$, all being assigned to the k^{th} UE. For ZF, the equation is presented as:

$$\mathbf{G=H(H^HH)^{-1}} \qquad (7)$$

Where **H** is a matrix containing all UE channels $[\mathbf{h}_1, \mathbf{h}_2, \ldots, \mathbf{h}_k]$, The matrix G is used to eliminate interference from other users. HH means that all the user channels fading are insignificant and are evenly distributed between the uplink and downlink, while the inverse operation means channel equalization between uplink and downlink. σ^2 denotes the noise variance (in Joule's symbol), $\mathbf{p}^{(ul)}$ is diag $(\mathbf{p}^{(ul)}_1, \mathbf{p}^{(ul)}_2, \ldots, \mathbf{p}^{(ul)}_k)$, and the design parameter $p^{(ul)}_i \geq 0$ Which is the transmitted uplink power of UE i (in Joule/symbol) for i= 1, 2,....,K.

Similarly, for downlink transmissions, ZF being the precoding schemes is considered, this is denoted by $\mathbf{V} = [\mathbf{v}_1, \mathbf{v}_2, \ldots, \mathbf{v}_k] \in C^{MxK}$ the precoding matrix for ZF is also used for downlink data transmission. The precoding matrix V is derived in a similar way:

$$\mathbf{V=H(H^HH)^{-1}} \qquad (8)$$

Comparing equations (7) and (8), it is natural to set V= G, thus reducing the computational complexity as it may not be necessary. This system is designed to guarantee a uniform gross rate R^- (in bit second) for any active UE, where $\zeta^{(ul)}\mathbf{R}^-$ is the uplink rate and $\zeta^{(dl)}\mathbf{R}^-$ is the downlink rate. This feat would be achieved by the combination of the linear processing and proper power allocation.

At the Uplink, the following is expected to be achieved from the assumptions of Gaussian codebooks, linear processing, and perfect CSI, the expected uplink rate (in bit/second) of the k^{th} UE is presented as:

$$R_k^{(ul)} = \zeta^{(ul)}\left(1 - \frac{\tau^{(ul)}k}{U\zeta^{(ul)}}\right)\hat{R}_k^{(ul)} \quad (9)$$

Where the pre-log factor (1- $\tau^{(ul)}$k/ u$\zeta^{(ul)}$) accounts for pilot overhead and $\zeta^{(ul)}$ is the fraction of uplink transmission.

$$\hat{R}_k^{(ul)} = B_{log}\left(1 + \frac{p_k{}^{(ul)}\left|g^H_{kh_k}\right|^2}{\sum_{l=l,l=k}^{k} p_l^{(ul)}\left|g^H_{kh_k}\right|^2 + \sigma^2\|g_k\|^2}\right) \quad (10)$$

In addition, the uplink gross rate (in bit second) from the *kth* UE, where "gross" refers to, indicate that the overhead factors are not included. As earlier mentioned, the aim is to provide the same gross rate $R_k^{-(ul)}$ is R^- for k=1,2…, K. This condition can be met if the uplink power allocation vector $P^{(ul)}$ is $[P_1^{(ul)}, P_2^{(ul)}, \ldots, P_k^{(ul)}]^T$. This is presented as:

$$P^{(ul)} = \sigma^2\left(D^{(ul)}\right)^{-1} 1_k \quad (11)$$

This indicates that the power allocation $P^{(ul)}$ depends on the inverse of the matrix $D^{(ul)}$ and the noise variance σ^2. Uplink power allocation vector specifies the transmit power for each of the K UEs in the system and ensures uniform gross rate across UEs.

where the (k, l) the element of $D^{(ul)} \epsilon C^{kxk}$ is

$$\left[D^{(ul)}\right]_{k,l} = \begin{cases} \frac{\left|g^H_{kh_k}\right|^2}{(2^{R/B}-1)\|g_k\|^2} - \frac{\left|g^H_{kh_l}\right|^2}{\|g_k\|^2} & \text{for } k = l \;\&\; for\; k \neq l \end{cases} \quad (12)$$

The equation (11) is the direct computation of power allocation in ZF detection, the average uplink power (PA) (Watt) is given as the power consumption of the power amplifiers (PAs), which entails the radiated transmit power and the PA dissipation. This definition can be implemented using equation (11), this can be obtained as:

$$P_{\mathrm{Tx}}^{(ul)} = \frac{\mathrm{B}\zeta^{(\mathrm{ul})}}{\eta^{(\mathrm{ul})}} E\{1_k^{\mathrm{T}} P^{(ul)}\} = \sigma^2 \frac{B\zeta^{(ul)}}{\eta^{(ul)}} E\left\{1_k^{\mathrm{T}}\left(D^{(ul)}\right)^{-1} 1_k\right\} \quad (13)$$

where $0 < \eta^{(ul)} \leq 1$ is the PA efficiency at the UEs. It can be observed that $\hat{R}$ cannot support any transmit power. In this scenario, the computation for $P^{(ul)}$ in equation (11) would give answers in negative powers, this can however be easily detected and also can be avoided by computing the spectral radius $D^{(ul)}$. This can only happen in interference-limited scenarios; this problem would not manifest if ZF is implemented under perfect CSI. Under these conditions, $P_{TX}^{(ul)}$ in the equation can be derived in closed form.. Therefore optimizing the parameters like $P^{(ul)}$, $D^{(ul)}$, in Equation (13) is key to achieving a balance between fairness, throughput, and energy savings in the entire system. In a situation where ZF detector is used with $M \geq K + 1$, the gross rate without losing the generality can be expressed as:

$$\hat{R} = B_{log(1+\rho^{(M-K)})} \quad (14)$$

Where ρ is a design parameter that is proportional to the received SINR. The PA power $P_{TX}^{(ul-ZF)}$ required to ensure that each UE encounters little or no loss in its gross rate in equation (14) is represented as:

$$P_{TX}^{(ul-ZF)} = \frac{\mathrm{B}\zeta^{(\mathrm{ul})}}{\eta^{(\mathrm{ul})}}\sigma^2 \rho S_x K \quad (15)$$

Where $S_x = E_{x(1-(X))-1}$ accounts for user distribution and propagation environment under perfect CSI.

Downlink: AT The downlink, the signal of the k^{th} UE is assigned a transmit power of $P_k^{(dl)}$ (in Joule/ symbol) and this is also normalized by a precoding vector $V_k \| V_k \|$. With assumptions from Gaussian codebooks and perfect CSI, the attainable downlink rate (in bit second) of the *kth* UE with linear processing is expressed in terms of R as:

$$R_k^{(dl)} = \zeta^{(dl)}\left(1 - \frac{\tau^{(dl)}K}{U\zeta^{(dl)}}\right)\hat{\mathrm{R}}_k^{(dl)} \quad (16)$$

Where $\left(1 - \frac{\tau^{(dl)}K}{U\zeta^{(dl)}}\right)$ the downlink is pilot overhead and $\hat{\mathrm{R}}_k^{(dl)}$ is the gross rate (in bit/second).

The gross rate at the downlink is expressed mathematically as:

$$R_k^{(dl)} = Blog\left(1 + \frac{P_k^{(dl)}\frac{|h_k^H v_k|^2}{\|v_k\|^2}}{\sum_{l=1,l\neq k}^{K} P_l^{(ul)}\frac{|g_k^H v_l|^2}{\|v_l\|^2} + \sigma^2}\right) \quad (17)$$

Where the average PA power is defined or expressed in equation form as:

$$P_{\mathrm{TX}}^{(dl)} = \frac{B\zeta^{(dl)}}{\eta^{(dl)}}\sum_{k=1}^{k} E\left\{P_k^{(dl)}\right\} \quad (18)$$

Where $0 < \eta^{(dl)} \leq 1$ is the PA efficiency at the BS

If the equal-rate condition $\hat{\mathrm{R}}_k^{(dl)} = \hat{\mathrm{R}}$ for all k, and the power allocation vector $P^{(dl)} = [P_1^{(dl)}, P_2^{(dl)}, \ldots\ldots, P_k^{(dl)}]^T$, which can be represented as $P^{(dl)}$ is $\sigma^2\left(D^{(dl)}\right)^{-1} 1_k$ where the $(k,l)ht$ element of $D^{(dl)} \epsilon c^{kxk}$ is

$$\left[D^{(dl)}\right]_{k,l} = \frac{|h_k^H v_k|^2}{(2^{R/B})\|v_k\|^2} - \frac{|h_k^H v_l|^2}{\|v_l\|^2} \text{ for } k = 1 \text{ and } k \neq 1 \quad (19)$$

Putting $P^{(dl)} = \sigma^2\left(D^{(dl)}\right)^{-1} 1_k$ into equation (19), the average downlink PA power (in watt) is presented as:

$$P_{TX}^{(dl)} = \sigma^2 \frac{B\zeta^{(dl)}}{\eta^{(dl)}} E\left\{1_K^T\left(D^{(dl)}\right)^{-1} 1_k\right\} \quad (20)$$

From equations (19) and (20), $D^{(dl)}$ is equal to $\left(D^{(ul)}\right)^T$ since ZF precoding is used with $M \geq K+1$, then the average downlink PA power $P^{(dl-ZF)_{TX}}$ require to serve each UE with a gross rate equal to $\hat{R}$ in equation (20) is expressed as:

$$P_{TX}^{(dl-ZF)} = \frac{B\zeta^{(dl)}}{\eta^{(dl)}} \sigma^2 \rho S_x K \quad (21)$$

The average uplink and downlink PA powers summed as presented in the equation (22) as follows:

$$P_{TX}^{(ZF)} = P_{TX}^{(ul-ZF)} + P_{TX}^{(dl-ZF)} = \frac{B\sigma^2 \rho S_x}{\eta} K \quad (22)$$

Efficiency: Efficiency under ZF processing is given as:

$$\eta = \left(\frac{\zeta^{(ul)}}{\eta^{(ul)}} + \frac{\zeta^{(ul)}}{\eta^{(ul)}}\right)^{-1} \quad (23)$$

The matrix size for zero forcing (ZF) can be derived from equation (22), then, the combining vector V^{ZF} is given as:

$$V^{ZF} = \hat{H}\left(\left(\hat{H}\right)^H \hat{H}\right)^{-1} \quad (24)$$

This is a force inverse of $\left(\hat{H}\right)^H$. The combination $\left(\hat{H}\right)^H$V of this combining scheme (ZF), the *kth* UE in a given cell network with interference element denoted by (k,i), within the same network with BS and UEs, where the EU_k interferes with UE, all in the same network, for $K = l$ then the combining vector is expressed as:

$$\left(\hat{H}\right)^H V^{ZF} = \left(\hat{H}\right)^H \dot{H}((\hat{H})\text{^}H\ \hat{H})\ )^{-1} \quad (25a)$$

$$\left(\hat{H}\right)^H V^{ZF} = I_k \quad (25b)$$

I_k an identity matrix implies that the interference from intra cell UEs is cancelled, while the transmitted signal remains at unity or non-zero, hence V^{ZF} is a K+K matrix.

The Energy Efficiency EE is defined as the amount of information reliably transmitted per unit of energy, which is measured in (bit/Joule), is mathematically expressed as explained by Pizze *et al.* (2012) as follows:

$$EE = \frac{Area\ throughput\left(\frac{bit/s}{km^2}\right)}{Area\ power\ consumption\left(\frac{W}{km^2}\right)} = \frac{Bw(Hz).ASE\left(\frac{\frac{bit}{s}/Hz}{km^2}\right)}{Apc\left(\frac{W}{km^2}\right)} \quad (26)$$

Where Bw is the Bandwidth, ASE is the Area Spectral Efficiency, and APC is the Area power consumption

3. RESULTS

3.1 Simulation Parameters

International telecommunication Union in charge of Radio Frequency (ITU-R) provided the standard equipment configurations for Massive MIMO technology employing Enhanced Mobile Broadband (eMBB) for dense metropolitan areas, which provided the data used in this study. This is to ensure that this study is aligned with the international benchmark. This study used the radio frequency (RF) architecture, the beamforming technique, and multiple arrays of smart antennas at the transmitter and receiver sides to detect and send multiple signals simultaneously from multiple desired terminals. Wavelet-Massive MIMO technology is the focus of this research. For the modeling and simulation of the 5G network using Massive MIMO system, it was executed by MATLAB. Both the graphs and analysis were generated from the analyzed data generated from the simulation.

Table 1: Network Simulation Parameter I

Parameter	**Value**
Network layout (NL)	25
UE antenna height	1.5m
Inter-BS distance	200 m
Maximum BS transmit power	44dBm
Maximum UE distance	35m
Channel model BS antenna height	25m
Minimum UE distance	35m
Maximum UE transmit power	23dBm
UE dropping (K)	6 UEs in 200m x 200m area per BS
Carrier frequency	4 GHz
Transmission Bandwidth (B)	20 MHz

(International Telecommunication Union (ITU), 2023)

Table 2: Network Simulation Parameter II

Parameter	**Value**
Backhaul Traffic Power (P_{BT})	0.25 W (Gbit/s)
Decoding power of data signals (P_{DEC})	0.8 W (Gbit/s)
Coding power of data signals (P_{COD})	0.1 W (Gbit/s)
Circuit component power at UE (P_{UE})	0.1 W
Circuit component power at BS (P_{BS})	1 W
Local oscillator power at BSs (P_{SYN})	2 W
Fixed power consumption (P_{FIX})	18 W
PA efficiency at the UEs ($\boldsymbol{\eta}^{(ul)}$)	0.3
PA efficiency at the BSs ($\boldsymbol{\eta}^{(dl)}$)	0.39
Computational efficiency at the UE (L_{UE})	5 Gflops/W
Computational efficiency at the BS (L_{AS})	12.8 Gflops/W
Relative pilot lengths ($\tau^{(ul);}\ \tau^{(ul)}$)	1
Total noise power ($B\sigma^2$)	-96 dBm

Channel coherence time (T_C)	10 ms
Channel coherence bandwidth (B_C)	180 KHz

(Bjornson *et al.*, 2015)

3.2 Massive MIMO Simulation Results

Both Massive MIMO technologies (i.e. W-OFDM and FFT-OFDM) were simulated over an urban channel with path loss component set at 3.75. The antenna arrays M was simulated over a range of values ranging from minimum of 6 antenna elements, 12 antenna elements, up to 96 antenna elements. This implies that 16 different Massive MIMO antenna setups were achieved for each base station (BS). The M values are the same for both Uplink and Downlink setups. Each base station (BS) range is 200 meters and it was down for one square kilometer, resulting to 25 different BS was assumed to be a square (This was assumed for easy computation).The number of virtual set ups was 4, while the number of random realizations was 10. The number of user equipment (UE) was set at 6 users per base station (BS) as earlier stated, thereby making the total UE per square kilometer to 150. The minimum distance separating each UE was 35 meters. Other setup parameters are summarized in Table 1 for the Massive MIMO simulation.

3.3 Sum Spectral Efficiency

The results gotten from the spectral efficiency of each cell within the simulated network for the Wavelet-OFDM Massive MIMO during the transmission of data to UEs are represented in Table 4. This average sum was resulted from the complex random realization during the simulation. Where each of the 25 network cells were subjected to different user equipment (UE) position and its spectral efficiencies taken, summed up then averaged for easy tabulation and for further evaluation. The values of spectral efficiency ranges from 4.9545 bits/s/Hz/cell when M antenna element is at 6 to 31.4297 bits/s/Hz/cell when M antenna element is at 96.

Table 3: Network System Parameters for Massive MIMO Network Simulation

Parameter	Value
Network Layout	Square
Number of Network Cells	25
Cell Distance	200 meters
Range of Antenna per BS	10 to 100 antenna element
Number of UE's per Cell	10
Channel gain per KM	-148.1 Db
Pathloss Exponent	3.76
Shadow Fading	10
Bandwidth	20 MHZ
Receiver Noise power	-94 dBm
Uplink Transmit Power	20 dBm
Downlink Transmit Power	20 dBm
Samples per Coherent Block	200
Pilot Reuse Factor	1

Table 4: Sum Spectral Efficiency for Wavelet-OFDM from MATLAB

Antenna (M)	6	12	18	24	30	36
Average Sum SE (bits/s/Hz/cell)	4.9545	7.7052	12.7273	16.0868	18.5372	20.4318
Antenna (M)	42	48	54	60	66	72
Average Sum SE (bits/s/Hz/cell)	22.3452	23.6747	24.9464	25.9833	27.2498	28.1923
Antenna (M)	78	84	90	96		
Average Sum SE (bits/s/Hz/cell)	28.9088	30.1074	30.6088	31.4297		

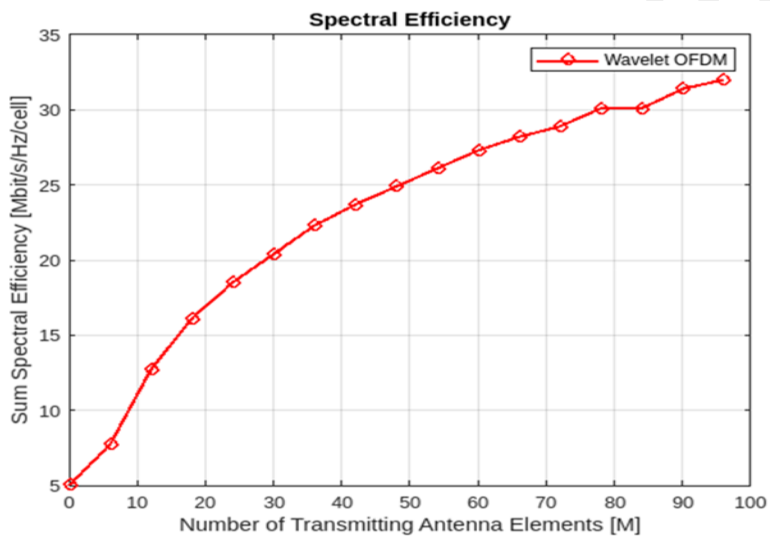

Fig. 1: Sum Spectral Efficiency against Number of Antenna Element in Wavelet-OFDM Massive MIMO Network

The graphical representation of the sum spectral efficiency plotted against the number of different ranges of antenna elements within the simulation during the transmission of data to EUs and vice versa is illustrated in Figure 1. The average sum SE is at its lowest value when the transmission antenna elements M is 6 then increases sharply when M is at 24, then a gradual growing curve when M is set at 30 up to 96.

3.4 Energy Efficiency

The Energy Efficiency data is plotted against the number of different ranges of antenna elements within the simulation during transmission and reception of data's to UEs and vice versa and are presented in Table 5.

Table 5: The Energy Efficiency for Wavelet-OFDM Massive MIMO Network

Antenna (M)	6	12	18	24	30	36
Energy Efficiency (Mbits/Joule/cell)	3.2754	4.2567	5.9108	6.5018	6.6325	6.5572
Antenna (M)	42	48	54	60	66	72
Energy Efficiency	6.4999	6.2968	6.1104	5.8971	5.7605	5.5767

(Mbits/Joule/cell)				
Antenna (M)	78	84	90	96
Energy Efficiency (Mbits/Joule/cell)	5.3725	5,2747	5.0720	4.9395

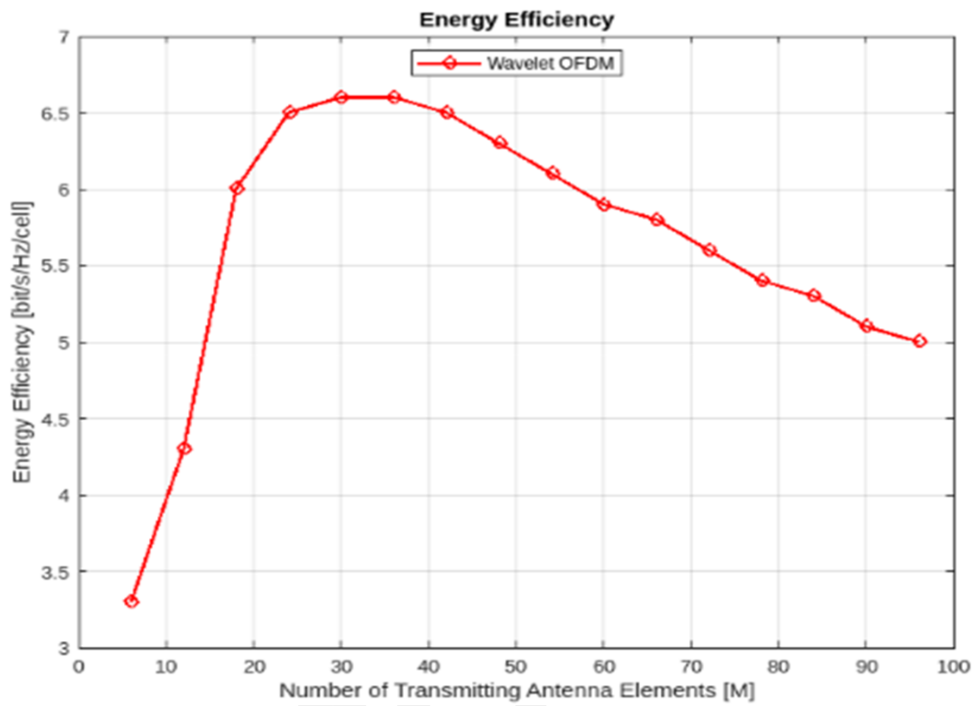

Fig. 2: Energy Efficiency of the Simulations for Massive MIMO Network

Figure 2 shows a unique characteristic plot where each antenna element value relationship with the energy efficiency is different. From Figure 2, the energy efficiency is at its lowest value 3.27540 Mbit/Joule/cell when the antenna elements M is 6 then increases sharply to 6.5018 Mbit/Joule/cell, when M is at 24, then a gradual growing curve to its peak value of 6.6325 Mbit/Joule/cell when M is set at 30. A slightly decreasing curve of value 6.4999 Mbit/Joule/cell, when M is 42 is observed. From M equal to 42 with value 6.4999 Mbit Joule cell to M equal to 96 with value 4.9395 Mbit/Joule/cell, it was observed that there is a constant decay in the energy efficiency value.

3.5 Energy Efficiency versus Spectral Efficiency

The antenna, sum spectral efficiency, and energy efficiency of the wavelet-OFDM Massive MIMO network simulation are presented in Table 6. The values for M antenna elements range from 6 to 96, for energy efficiency from 3.2754 Mbit/Joule/cell to 4.9395 Mbit/Joule/cell, and for spectral efficiency from 4.9545 bit/s/Hz/cell to 31.4297 bit/s/Hz/cell. The energy efficiency of the massive MIMO network is plotted versus its spectral efficiency in Figure 3. As is already known, this graph represents the Wavelet-OFDM Massive MIMO network's spectrum efficiency and energy efficiency per cell. It is observed that the energy efficiency varies with spectral efficiency. At 4.9545 bit/s/Hz/cell, it is at its lowest value of 3.2754 Mbit/Joule cell. At 16.0868 bit/s/Hz/cell, it increases sharply to 6.5018 Mbit/Joule/cell. A gradual growing curve then reaches its peak value of 6.6325 Mbit/Joule cell. When the spectral efficiency is 20.4318 bit/s/Hz/cell, a slightly declining curve with a value of 6.5572 Mbit/Joule/cell is found. After that, there is a gradual decline until the efficiency is 4.9395.

Table 6: Energy Efficiency versus Spectral Efficiency Wavelet-OFDM

Antenna (M)	**6**	**12**	**18**	**24**	**30**	**36**
Sum SE (bits/s/Hz/cell)	4.9545	7.7952	12.7273	16.0868	18.5372	20.4318
Energy Efficiency (Mbits/Joule/cell)	3.2754	4.2567	5.9108	6.5018	6.6325	6.5572
Antenna (M)	**42**	**48**	**54**	**60**	**66**	**72**
SE (bits/s/Hz/cell)	22.3452	23.6747	24.9464	25.9833	27.2498	28.1923
Energy Efficiency (Mbits/Joule/cell)	6.4999	6.2968	6.1104	5.8971	5.7605	5.5767
Antenna (M)	**78**	**84**	**90**	**96**		
SE (bits/s/Hz/cell)	28.9088	30.1074	30.6088	31.4297		
Energy Efficiency (Mbits/Joule/cell)	5.3725	5,2747	5.0720	4.9395		

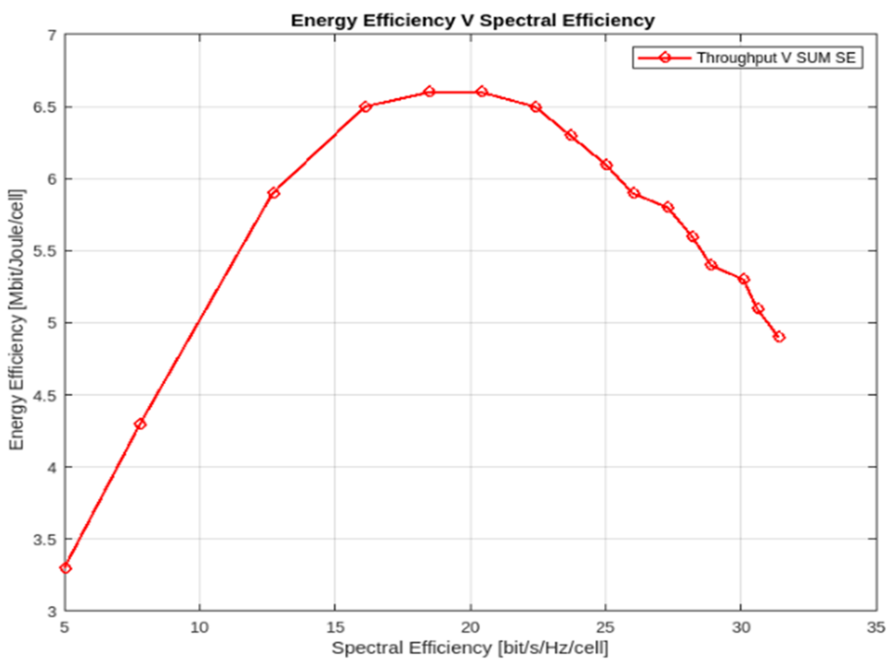

Fig. 3: Energy Efficiency versus Spectral Efficiency for Wavelet-OFDM

3.6 Comparison of Wavelet-OFDM against FFT-OFDM Massive MIMO System

In the simulation, during data transmission to UEs and vice versa, Figure 4 shows the graphical depiction of the comparison for a spectrum efficiency plotted against the member of various ranges of antenna elements. The average sum of the squared errors (SE) is at its minimum when the transmitting antenna elements (M) have a value of 6. It then rises quickly when M has a value of 24, and then gradually when M has a value of 30 up to 96. This is true for every scheme under comparison. The Wavelet-based Massive

MIMO system outperformed all others on the graph, with the EFT-OFDM Massive MIMO setup performing the worst with a 20% cyclic prefix.

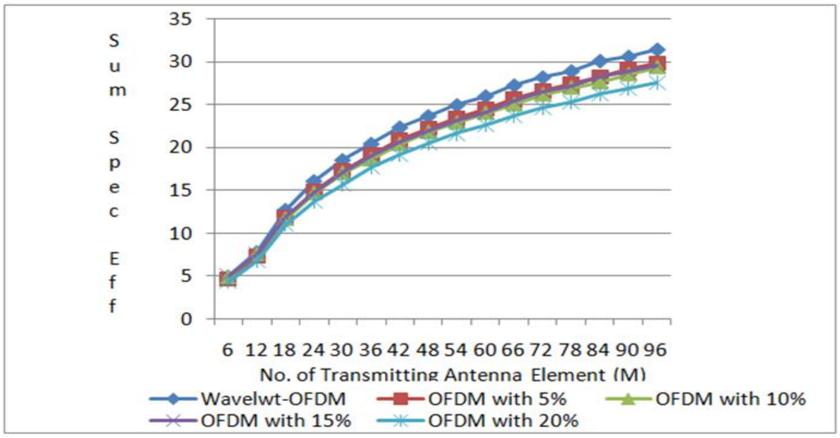

Fig. 4: Comparison for Spectral Efficiency

3.7 Energy Efficiency Comparison

The Energy Efficiency of the various Massive MIMO networks simulated for these comparisons is plotted graphically in Figure 5. As it may already know, this graph is derived from the total circuit power consumption per cell and the data throughput per cell, which are both computed over the speed for these throughput values across the various antenna elements for Massive MIMO networks. The Energy Efficiency data is plotted against the number of different ranges of antenna elements within the simulation during data transmission and reception to UEs, and vice versa. Figure 5 features a unique characteristic plot where each antenna element value is different from the energy efficiency. The Wavelet-based Massive MIMO setup had the best performance on the graph, whereas the FFT-OFDM Massive MIMO setups with 20% cyclic prefix performed the worst, as shown in Figure 5.

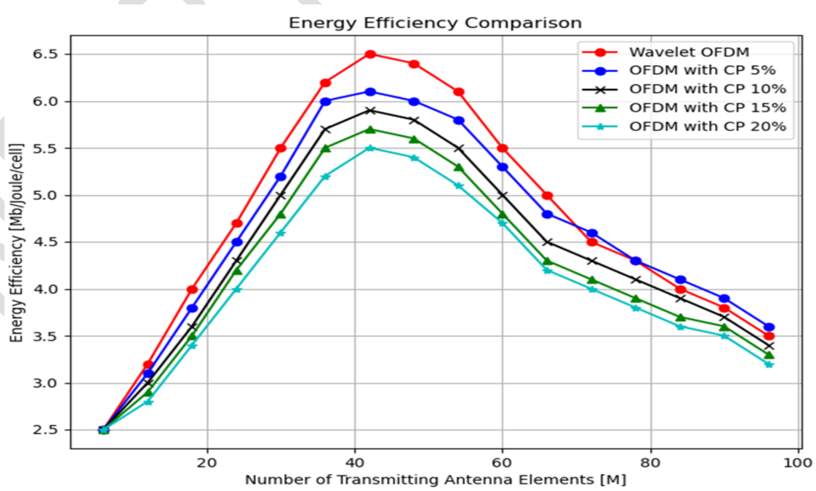

Fig. 5: Energy Efficiency Comparison

3.8 Energy and Spectral Efficiencies Comparison

With varying degrees of cyclic prefix (CP) inserted, the energy efficiency against spectral efficiency for the comparison of Wavelet-OFDM and FFT-OFTD Massive MIMO networks is graphically represented in

Figure 6. As previously said, this graph is a plot of the energy efficiency for each of the simulated schemes versus the spectral efficiency of each scheme. It starts with the derivation of the uplink and downlink average sum spectral efficiencies computed over the specified bandwidth for its throughput. Figure 6 shows that the Wavelet-based Massive MIMO system outperformed all others, with the FFT-OFDM Massive MIMO setup doing the worst with a 20% cyclic prefix.

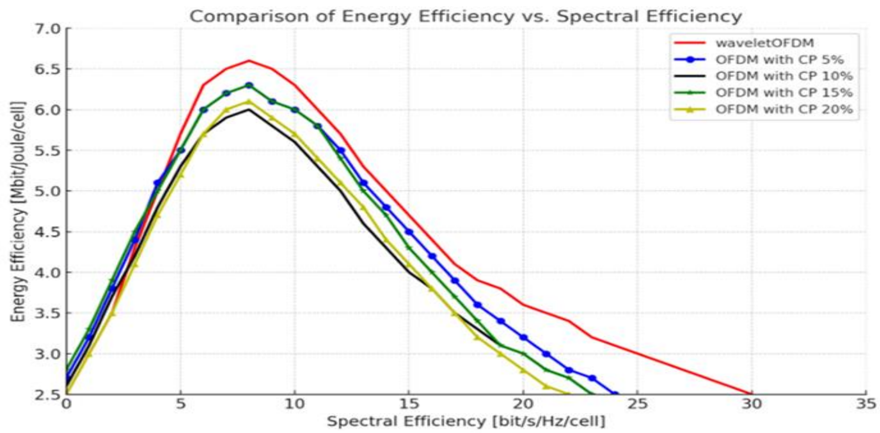

Fig. 6: Comparison for Energy Efficiency versus Spectral Efficiency

3.9 Energy and Spectral Optimization Process

A decreasing trend was seen in the graphs for Spectral Efficiency and Energy Efficiency against M number of antennas, and Energy Efficiency; as a result, several standout peaks needed to be chosen for assessment. In order to facilitate identification, three peak points were chosen and displayed in a bar chart. The bar chart in Figure 7 illustrates the three (3) highest energy efficiency values vs the appropriate number of antennas for the complete simulated design. The Wavelet-based Massive MIMO system outperformed all others in this graphic, with the FFT-OFDM Massive MIMO setup with 20% cyclic prefix performing the worst. However, for all the Energy-efficient designs, M at 24 has the lowest figure at their corresponding antenna element number, followed by M at 36, and M at 30 has the greatest figure.

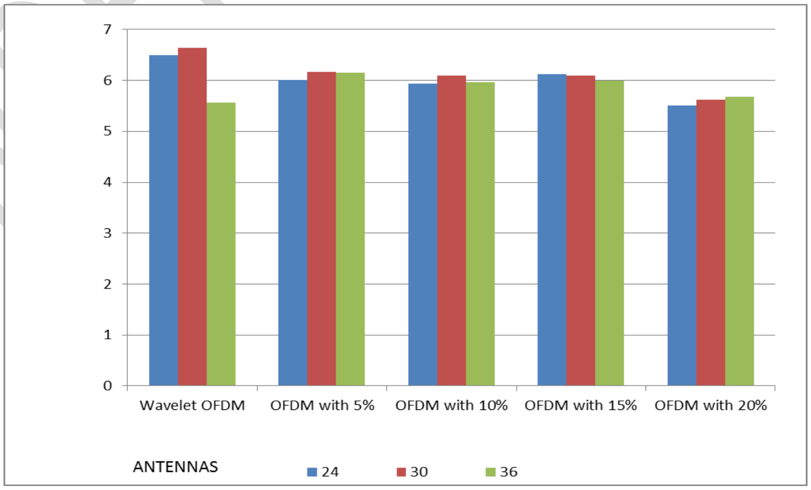

Fig.7: Comparison for Energy Efficiency against Antenna

Figure 7 shows the three (3) maximum Energy Efficiency values for each Spectral Efficiency related to the number of antennas throughout the full simulated system. The Wavelet-based Massive MIMO system outperformed all others in this graphic, with the FFT-OFDM Massive MIMO setup with 20% cyclic prefix performing the worst. However, for all the schemes for the spectral efficiency, M at 24 has the lowest result, followed by M at 30, and M at 36 has the highest figure. This indicates that when the number of antenna elements rises, the spectral efficiency also increases.

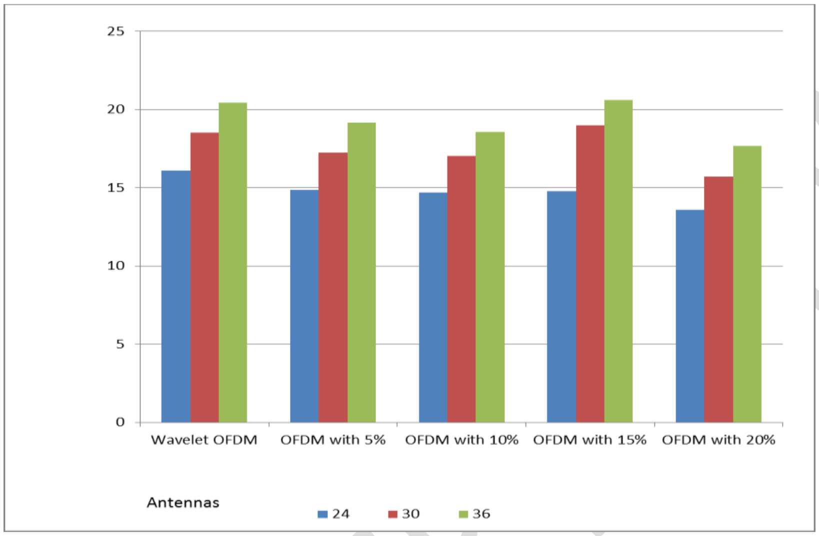

Fig. 8: Comparison for Spectral Efficiency against Antenna

4. DISCUSSION OF RESULTS

The spectral efficiency versus antenna numbers M graph is a right-side open parabola. This means that as the number of antenna M increases, the function initially accelerates slowly before speeding up quickly and eventually approaching a maximum value. The parabola opens to the right, with the vertex denoting the parabola's lowest point on the x-axis. This graph implies that the higher the number of antenna elements M, the higher the spectral efficiency of the communication systems.

The overall mean value of the spectral efficiency gotten in this research is 22.05 Bit/Sec/Hz/Cell which is closely related to the works of; Boumard *et al.* (2018), Jun and Heung (2018) and that of Usama and Erol-Kantarci (2019) who got their overall mean values at 21.55 bit/s/Hz, 22.03 bit/s/Hz and 21.99 bit/s/Hz respectively. The slight changes in the values are due majorly to the fact that they used frequency reuse and channel coding methods to improve the spectral efficiency through the MIMO antennas and the cell distance is 180meters instead of 200 meters in this research.

It is clearly observed that the energy efficiency is at its lowest value of 3.27540 Mbit/Joule/cell when the antenna elements M is 6, it then increases sharply to 6.5018 Mbit/Joule/cell, when M is at 24, then a gradual growing curve to its peak value of 6.6325 Mbit/Joule/cell when M is set at 30. A slightly decreasing curve of value 6.4999 Mbit/Joule/cell, when M is 42 is observed. From M equal to 42 with value 6.4999 Mbit Joule cell to M equal to 96 with value 4.9395 Mbit/Joule/cell, it was observed that there is a constant decay in the energy efficiency value.

Wavelet-OFDM (W-OFDM) offers notable advantages over traditional FFT-OFDM in massive MIMO systems, primarily due to its superior spectral efficiency, interference resilience, and computational efficiency. By utilizing wavelet-based filters, W-OFDM reduces out-of-band emissions, allowing closer placement of channels and thus enhancing spectral efficiency. It also adapts better to frequency-selective fading and interference, making it more robust in urban environments with dense scatterers. Additionally, the multiresolution nature of wavelets enables more efficient processing, which is beneficial in high-capacity networks where power and computational resources are constrained. These properties make W-OFDM particularly advantageous in dense, high-mobility scenarios, offering a viable improvement over FFT-OFDM for future-generation networks. It is therefore crucial for science, engineering, and design technicians to comprehend the energy efficiency behavior under these numbers of antenna elements M. As such, this behavior warrants additional investigation, particularly in the nonlinear region down to a threshold that is comparable to the breaking point.

5. CONCLUSION

The analytical assessment of W-OFDM mMIMO for enhancing spectral and energy efficiencies in wireless digital telecommunication system shows encouraging outcomes and a substantial potential for network capacity and efficiency. The results of the study indicate that W-OFDM mMIMO may successfully meet the growing needs of contemporary communication environments for high spectrum and less energy consumption. The simulation results provide important new information about W-OFDM mMIMO network performance characteristics. In terms of spectral and energy efficiencies, the designed system performed better than earlier systems when compared to different FFT-based OFDM schemes. When the energy efficiency reached its maximum, with M antenna element at 30 and constant UEs at 6, the system was further optimized. The result of this unique system is promising since it outperformed previously existing systems.

This study uniquely contributes to the field of communication systems by thoroughly examining the relationship between spectral and energy efficiencies across varying antenna counts in Massive MIMO setups. By presenting empirical findings on spectral efficiency, which show an average of 22.05 Bit/Sec/Hz/Cell, it demonstrates how incremental increase in antenna numbers impact efficiency metrics, accelerating up to a peak before tapering. Notably, this research analyzes a range of antenna elements from 6 to 96, providing insights into the non-linear decay of energy efficiency at higher counts, a lesser-explored area in existing literature. This detailed analysis highlights practical implications for engineers, particularly regarding optimal antenna deployment, and opens further research avenues by emphasizing the need for deeper exploration in non-linear efficiency behaviors under increasing antenna loads.

Further investigation could involve the application of advanced modulation schemes and hybrid beamforming techniques to enhance performance in ultra-dense environments. Additionally, examining the robustness of Wavelet-OFDM under diverse propagation conditions such as high mobility or interference-prone areas could provide insights into its practical feasibility in 5G and beyond. Moreover, expanding to different frequency bands, such as mmWave or sub-THz, and analyzing the impact of channel conditions on energy consumption and throughput would be valuable. These areas of inquiry could significantly benefit scholars and practitioners by identifying methods to achieve optimal performance across varied deployment scenarios.

Disclaimer (Artificial intelligence)

Option 1:

Author(s) hereby declare that NO generative AI technologies such as Large Language Models (ChatGPT, COPILOT, etc.) and text-to-image generators have been used during the writing or editing of this manuscript.

REFERENCES

Agboje, O. E., Idowu-Bismark, O. B. & Ibhaze, A. E. (2017). Comparative analysis of fast fourier transform and discrete wavelet transform based MIMO-OFDM. *Int. J. Commun. Antenna Propag*, *7*(2), 168.

Ahmad, M. & Shin, S. Y. (2023). Wavelet-based massive MIMO-NOMA with advanced channel estimation and detection powered by deep learning. *Physical Communication*, *61*(1), 102189.

Badic, B., O'Farrell, T., Loskot, P. & He, J. (2010). Effect of the Base Station Antenna Beam Tilting on Energy Consumption in Cellular Networks. In *2010 IEEE 72nd Vehicular Technology Conference-Fall* (pp. 1-5). IEEE.

Boccardi, F., Andrews, J., Elshaer, H., Dohler, M., Parkvall, S., Popovski, P. & Singh, S. (2016). Why to Decouple the Uplink and Downlink in Cellular Networks and how to do it. *IEEE Communications Magazine*, *54*(3), 110-117.

Chataut, R. & Akl, R. (2020). Massive MIMO Systems for 5G and Beyond Networks—Overview, Recent Trends, Challenges, and Future Research Direction. *Sensors*, *20(*10), 2753.

Donzelli, E., Salvade, A., Mimo, P., Viganò, M., Morrone, M., Papagna, R. & Tredici, G. (2007). Mesenchymal Stem Cells Cultured on a Collagen Scaffold: In Vitro Osteogenic Differentiation. *Archives of Oral Biology*, *52*(1), 64-73.

Guo, J. (2014). Energy Efficiency in Wireless Networking Protocols. *current issues in Wireless and Mobile Networking. http://www. cse. wustl. edu/~ jain/cse574-14/index. html*.

Marr, B. (2012). *Key Performance Indicators (KPI): The 75 Measures Every Manager Needs to Know*, 7(1), 29-34.

Marzetta, T. L. (2010). Noncooperative Cellular Wireless with Unlimited Numbers of Base Station Antennas. *IEEE Transactions on Wireless Communications*, *9*(11), 3590-3600.

Marzetta, T. L. & Hochwald, B. M. (2006). Fast Transfer of Channel State Information in Wireless Systems. *IEEE Transactions on Signal Processing*, *54*(4), 1268-1278.

Ngo, H. Q., Larsson, E. G. & Marzetta, T. L. (2014). Aspects of Favorable Propagation in Massive MIMO. In *2014 22nd European Signal Processing Conference (EUSIPCO)*, 149 (1), 93-127.

Stuber, G. L., Barry, J. R., Mclaughlin, S. W., Li, Y., Ingram, M. A. & Pratt, T. G. (2004). Broadband MIMO-OFDM Wireless Communications. *Proceedings of the IEEE, 92*(2), 271-294.

Terré, M., Pischella, M. & Vivier, E. (2013). *Wireless Telecommunication Systems*. John Wiley & Sons. *Journal of Clean Energy Technologies*, 2(3), 12 - 15.

Terry, J. & Heiskala, J. (2002). *OFDM wireless LANs: A Theoretical and Practical Guide*. Sams publishing. *International Journal of Engineering Sciences & Research Technology,* 40(3), 4 -23.

Usama, M. & Erol-Kantarci, M. (2019). A Survey on Recent Trends and Open Issues in Energy Efficiency of 5G. *International Conference on Ubiquitous and Future Networks (ICUFN)*, *19*(14), 3126.

Wang, L., Ngo, H. Q., Elkashlan, M., Duong, T. Q. & Wong, K. K. (2015). Massive MIMO in Spectrum Sharing Networks: Achievable Rate and Power Efficiency. *IEEE Systems Journal*, *11*(1), 20-31.

Wang, Q., Hempstead, M. & Yang, W. (2006). A realistic power consumption model for wireless sensor network devices. In *2006 3rd annual IEEE communications society on sensor and ad hoc communications and networks* (Vol. 1, pp. 286-295). IEEE.

Zhang, D. & Zhang, D. (2019). Wavelet Transform: Fundamentals of Image Data Mining: Analysis, Features, Classification and Retrieval. Accessed on 28th April, 2019 from http://coursehero.com/file/14575755/joshua/.